2005 American Control Conference
June 8-10, 2005. Portland, OR, USA

Tip Steering for Fast Imaging in AFM

Sean B. Andersson
Division of Engineering and Applied Sciences
Harvard University, Cambridge, MA 02138
sanderss@deas.harvard.edu

Jiwoong Park
The Rowland Institute at Harvard
Harvard University, Cambridge, MA 02142
park@rowland.harvard.edu

Abstract— **In atomic force microscopy a sharp tip, supported by a cantilevered beam and interacting locally with a sample, is raster-scanned over a surface to build a three-dimensional image. Typical scan times are on the order of minutes or longer, depending on the size, resolution, and image quality desired. For a variety of reasons it is of great interest to reduce the time to gather an image. One of the most exciting applications is the imaging in real time of dynamic phenomena such as the motion of single molecules in molecular biology. In many cases the sample to be imaged is string-like, such as nanowires, actin, and DNA strands. In this case most of the imaging time is wasted gathering data about the substrate rather than about the sample. In this work we propose a high-level control algorithm to steer the tip along the string, thereby imaging only the area directly around the sample. This approach focuses the resolution directly where desired and greatly reduces the time to gather an image by reducing the area to be scanned. Depending on the sample, an order of magnitude or better improvement in the imaging time can be achieved. As the algorithm makes no demands on the low-level control of the tip it can be combined with approaches aimed at increasing the allowed scanning speed, resulting in even greater reductions in the imaging time. Furthermore, the chances of damaging the tip due to interaction with stray particles on the substrate is greatly reduced since the tip is kept near to the sample. In addition to a simulation study, we present a physical experiment in which a carbon nanotube is imaged using an atomic force microscope controlled by the tip-steering algorithm. To the authors knowledge this is the first reported instance of an image obtained by such high-level feedback control.**

I. Introduction

Scanning probe microscopy (SPM) is a class of atomic-scale imaging technologies in which a tip, interacting locally with a sample, is raster-scanned over the surface to build a three-dimensional image. A variety of different physical principles can be used for imaging. Examples include scanning tunneling microscopy (STM) which measures the electron tunneling current between the tip and the sample [4], near-field scanning optical microscopy (NSOM) which provides resolution beyond the diffraction limit of the illuminating light [8], atomic force microscopy (AFM) which measures the surface repulsion forces [3], and magnetic resonance force microscopy (MRFM) which measures the forces due to the magnetic nuclei in the sample [22]. Work in this area is ongoing and new technologies are continuing to be developed.

Because the measurement is local, the tip must be scanned over the surface and an image built over time. With the raster-scan pattern, typical imaging times can be on the order of several minutes or longer, depending on the size, resolution, and quality of image desired. While this long time delay is merely an inconvenience when imaging static structures, it is a fundamental problem when using SPM to investigate dynamic phenomena. Due to the wide variety and importance of such phenomena, particularly in molecular biology, it is of great interest to reduce the time to capture an image.

In this paper we focus on AFM as the target application. In AFM, a sharp tip, supported by a cantilevered beam, is brought in close contact with the sample and the deflection of the beam is measured. The microscope can be operated in several modes including contact (constant-height) mode, constant-force mode, and tapping mode. AFM is particularly well-suited for the investigation of biological structures because it requires no special material properties of the sample, it operates in liquid, and it has high spatial resolution [18]. A variety of methods have been proposed to reduce the imaging time in AFM. Most initial methods modified the design of the microscope such as using cantilevers with very high natural frequency [19] or controlling the quality factor of the probe [1], [13]. Commercial machines control the lateral and vertical motion of the tip utilizing simple PI control loops and recent work has used advanced feedback control to speed up the scanning system [7] and modern model-based control methods to increase the bandwidth of the AFM in the vertical direction [16], [17].

A few researchers have developed innovative techniques for imaging dynamic phenomena in molecular biology using an atomic force microscope, such as the transcription of DNA by RNA polymerase [9], [11]. Sequential AFM images, separated by between 37 seconds to 2 minutes, were compared to determine the activity of RNA polymerase. However, RNA polymerase has been shown to translocate along natural double stranded DNA templates at a maximal speed of between 12 and 19 bases per second during transcription [12] and thus this approach is far from imaging the transcription of a single base. In order to achieve this goal, new control techniques are needed.

Often the sample of interest has a structure which is string-like, including examples such as nanowires, DNA strands, actin strands, and microtubules. In this case, under the raster-scan approach much of the imaging time is wasted in obtaining data about the substrate rather than about the sample. In this work we seek to reduce the imaging time by using a high-level control algorithm to steer the tip along

0-7803-9098-9/05/$25.00 ©2005 AACC

the string. Modeling the sample as a planar curve, we seek to perform a "local" raster-scan by moving the tip along a line segment which is perpendicular to the curve in an appropriate sense as described in Section III. Using ideas from curvature-based control [10], [20], the next scan line is determined by estimating the next position of the frame from the current data.

This approach provides several benefits. The time to acquire an image is greatly reduced simply by reducing the total area that needs to be covered by the tip. Depending on the type of sample being imaged, an order of magnitude or better improvement in the scanning time can be expected. In addition, the approach reduces the likelihood of damage to the tip due to stray particles on the surface. Moving the tip over these large structures can easily damage the tip; by staying local to the string it is less likely that these structures will be encountered. Furthermore, the approach developed is a high-level algorithm which makes no demands on the low-level control of the tip. It can therefore be combined with other techniques to achieve even greater reductions in imaging time.

II. Basics of AFM

We give here a very basic description of AFM. See, e.g. [2], for a more detailed introduction. The basic structure of an atomic force microscope is shown in Figure 1. The system is fully actuated in x, y, z with most machines utilizing a separate actuator for the z direction. In addition many modern microscopes have an independent actuator to drive the tip for tapping mode (described below). The x, y, and z positions may be directly measured and fed back to the controller or may be controlled in an open loop fashion. When the tip is brought in proximity to the sample surface, interaction forces cause the supporting beam to bend. This deflection is measured through the use of an optical lever in which a laser beam is reflected off the cantilever and onto a split photo-diode. The controller itself is connected to a host computer which typically displays the data and sends scan parameters such as the scan size and scan speed as well as high level commands such as start and stop. In most commercial devices the low level controller implements a high-speed PI controller.

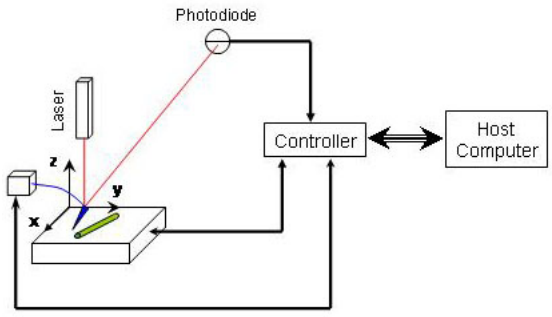

Fig. 1. Atomic force microscope schematic

Most images are acquired using one of three modes. In *contact* or *constant force* mode the tip is brought into stable contact with the sample. As the tip moves across the sample it is deflected up or down due to topographic variations in the sample. This deflection is directly measured by the microscope. The controller actuates the z-direction to maintain a constant deflection in the beam. Since the cantilever behaves as a linear spring, the interaction force can be determined from the deflection measurement. In *tapping* mode the tip is driven into near-resonance and then brought close enough to the sample so that it contacts the surface at the bottom of its oscillation cycle. Due to changes in the topography, the oscillation amplitude and phase are altered. The controller uses the output of the optical lever and actuates the $z-$ direction to maintain a constant oscillation amplitude. Because the tip is not in constant contact with the surface, lateral forces applied by the tip to the sample are kept small. This can be especially important when imaging soft biological samples both to prevent damage to the sample and to produce an accurate image. Similar to tapping mode, in *non-contact* mode the tip is once again driven into resonance. It is then brought close to, but not in actual contact with, the surface. The motion of the tip is influenced by the short range noncontact forces of the sample and topography is sensed by detecting changes in the tip motion. Because it requires a high resonance frequency, this imaging mode is used almost exclusively for imaging in air.

III. Local raster-scanning

We model the string-like sample as a planar curve whose spatial evolution is given by the dynamic equations for the Frenet-Serret frame. In the plane, this frame is defined by the tangent vector to the curve at a point and a choice of normal direction perpendicular to the tangent vector. Such a frame is shown in Figure 2 superimposed on an image of a DNA strand captured with an AFM operated in tapping mode.

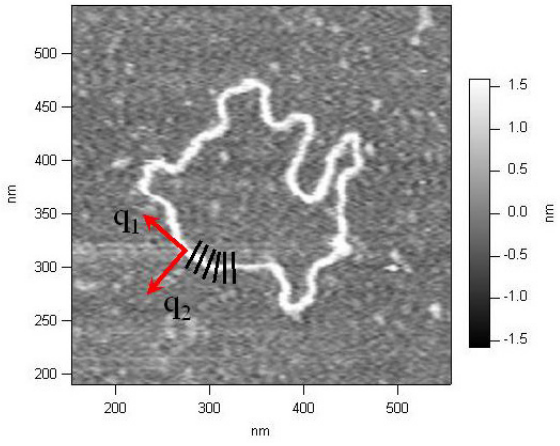

Fig. 2. Frenet-Serret frame superimposed on an AFM image of a DNA strand

Let s denote arclength along the curve. The equations of motion for the frame are given by

$$r'(s) = q_1(s), \quad (1a)$$
$$q_1'(s) = \kappa(s)q_2(s), \quad (1b)$$
$$q_2'(s) = -\kappa(s)q_1(s), \quad (1c)$$

where $r(s)$ is the point in the plane on the curve at arclength s, $q_1(s)$ and $q_2(s)$ are the tangent and normal vectors at s, $\kappa(s)$ is the curvature at s, and $'$ indicates derivative with respect to arclength. We assume that the initial conditions $r(0), q_1(0)$, and $q_2(0)$ are given.

To scan this sample we wish to imitate the raster scan motion but ensure that each scan line crosses the string perpendicular to the tangent vector q_1 and that the midpoints of each scan line lie on $r(s)$. Let v denote the desired scan speed and let a denote the desired width of the scan. If the underlying curve were known, then given a position $r(s)$ on the curve and the normal vector $q_2(s)$ at that point, the desired path of the tip is given by

$$\dot{x}(t) = \pm v q_2(s), \quad x(0) = r(s), \quad t \in \left[-\frac{a}{2v}, \frac{a}{2v}\right] \quad (2)$$

where the sign indicates the direction of crossing. We can then step forward a desired length Δ along the curve and repeat the process. This approach is illustrated in Figure 2. Because the image produced depends not only on the geometry of the sample but also the geometry of the tip and the direction of the scan over the sample, in most cases it is best to always scan the tip across the sample in the same direction rather than alternating scan directions despite the additional time this introduces.

The path of the underlying curve is of course not known a priori. It can however be estimated local to a point $r(s)$ given the current Frenet-Serret frame and the curvature at s by appealing to the spatial evolution equations in (1). We assume that κ changes slowly with respect to the step size Δ. The position $r(s)$ can be detected from the output of the AFM using a variety of estimation methods, depending on the type of sample being imaged. For example, one could utilize an observer-based sample detection scheme developed by Sebastian, Sahoo, and Salapaka [15] to rapidly detect the edges of the sample and then take $r(s)$ as either edge or as the midpoint.

Given estimates for two adjacent points on the string, $\hat{r}(s-\Delta)$ and $\hat{r}(s)$, the tangent vector $q_1(s)$ can be estimated using a simple finite difference approximation, that is

$$\hat{q}_1(s) = \frac{\hat{r}(s) - \hat{r}(s - n\Delta)}{\|\hat{r}(s) - \hat{r}(s - n\Delta)\|} \quad (3)$$

where $\|\cdot\|$ denotes the standard Euclidean metric. Here n is a fixed integer that can be chosen to offset difficulties arising from the small positional differences between points when the step size along the string is small. As the pair $q_1(s), q_2(s)$ are always orthogonal, $\hat{q}_2(s)$ is given by simply rotating $\hat{q}_1(s)$ by $\frac{\pi}{2}$ radians. Any noise in the measurement of $r(s)$ is of course amplified in this estimate of derivative.

To estimate the curvature we use a geometric approach based on Heron's formula (see [5] for a derivation and detailed description of the following). As in Figure 3, let A, B, C be three successive and nearby points on a curve and denote the Euclidean distances between the points as a, b, c respectively. The radius of curvature of the circle is

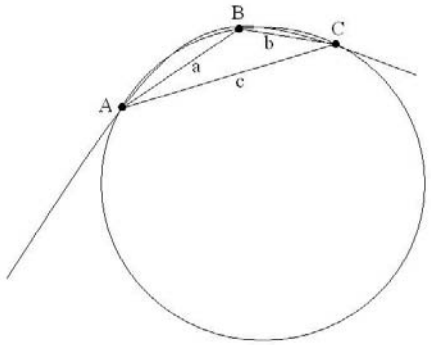

Fig. 3. Curvature approximation (from [5])

then

$$\kappa(A, B, C) = \pm 4 \frac{\sqrt{l(l-a)(l-b)(l-c)}}{abc} \quad (4)$$

where $l = \frac{1}{2}(a+b+c)$ is the semi-perimeter of the triangle. The estimate of the curvature of the string at the point $r(s)$ is given by (4) where the points A, B, C correspond to $r(s-2n\Delta), r(s-n\Delta)$, and $r(s)$ respectively where again n is a fixed integer. (See [21] for more information on curvature estimation.) The sign is positive if the cosine of the angle between the vector connecting the points $r(k-n)$ and $r(k)$ and the normal vector is positive (so that the normal vector points "inside" the curve).

Given these estimates of the parameters for the Frenet-Serret frame at the arclength s the next position $r(s+\Delta)$ and tangent vector $q_1(s+\Delta)$ can be estimated by solving (1). Since the curvature is assumed to change slowly with respect to the step size along the string, we may approximate it as constant along the interval Δ. The solution to (1) for fixed κ and for step size Δ is given by a simple application of the variation of constants formula. The resulting update equations are

$$r(s+\Delta) = \begin{cases} \frac{A_1(\kappa(s)\Delta)}{\kappa(s)} \begin{pmatrix} q_1(s) \\ q_2(s) \end{pmatrix} + r(s), & \kappa \neq 0 \\ q_1(s)\Delta, & \kappa = 0 \end{cases} \quad (5a)$$

$$\begin{pmatrix} q_1(s+\Delta) \\ q_2(s+\Delta) \end{pmatrix} = A_2(\kappa(s)\Delta) \begin{pmatrix} q_1(s) \\ q_2(s) \end{pmatrix} \quad (5b)$$

where

$$A_1(\theta) = \begin{bmatrix} \sin(\theta) & 0 & 1-\cos(\theta) & 0 \\ 0 & \sin(\theta) & 0 & 1-\cos(\theta) \end{bmatrix}$$

and

$$A_2(\theta) = \begin{bmatrix} \cos(\theta) & 0 & \sin(\theta) & 0 \\ 0 & \cos(\theta) & 0 & \sin(\theta) \\ -\sin(\theta) & 0 & \cos(\theta) & 0 \\ 0 & -\sin(\theta) & 0 & \cos(\theta) \end{bmatrix}$$

The basic algorithm described above is summarized as follows.

Algorithm 3.1: Local raster-scanning:

0. Initialize $r(0), q_1(0), q_2(0), \kappa(0)$, and set $k = 0$, $m = 1$.
1. Set $s = k\Delta$.
2. For $t \in \left[-\frac{a}{2v}, \frac{a}{2v}\right]$ control x as in (2)
3. Measure $r(s)$ and estimate $q_1(s), q_2(s), \kappa(s)$
4. Estimate the next position of the curve using (5)
5. Set $k = k + 1$ and go to 1.

While this algorithm is not sensitive to the initial conditions, it is necessary that the resulting first few scan lines cross the sample. In practice, the initial conditions could be determined in a variety of ways. For example, a standard raster-scan could be performed until a sample is detected. At that point the local raster-scan algorithm could be run.

To consider the reduction in imaging time possible using this algorithm, consider the DNA image in Figure 2. The image is approximately 500 nm square and thus, to obtain a 2 nm lateral resolution, 250 scan lines are required using the traditional raster-scan pattern. If the tip moves at 1 μm/s (2 lines per second) the image will require 125 seconds to obtain. The total length of the DNA strand in the image is roughly 1 μm. Moving in steps of 2 nm along the strand, 500 steps are required to image the entire DNA using the local raster-scan approach. DNA is only a few nanometers in diameter and to ensure each scan line fully crosses the strand, set each scan line to 20 nm in length. If the tip is moved at the same speed as during the traditional raster-scan then each line will take 20 ms to complete and thus the entire DNA strand will be imaged in only 10 seconds.

The algorithm relies on two main assumptions. First, the change in the curvature of the sample between each scan line must be small since the algorithm assumes it is constant over the step size Δ. If this assumption does not hold then the next predicted scan line will not cross the sample and the algorithm will fail. An example of this behavior in simulation is shown in Figure 4. To track highly varying curves, it is thus important that the step size remain small. However, such a step size is required to produce high resolution images and thus this assumption is not overly restrictive. In addition, one can increase the length of the scan line to ensure that the sample is crossed. However, as the length of the scan line increases it becomes more likely that other samples will be encountered and thus this approach must be handled with some care.

The second assumption is that the estimation of the center position of the sample is accurate. Any error in the measurement of $r(s)$ will be greatly amplified in the estimates of the tangent vector and curvature and the algorithm will not be able to track the sample. See [6] for additional comments along these lines. Detection and estimation techniques can be used to improve the estimate and make the algorithm more robust to noise.

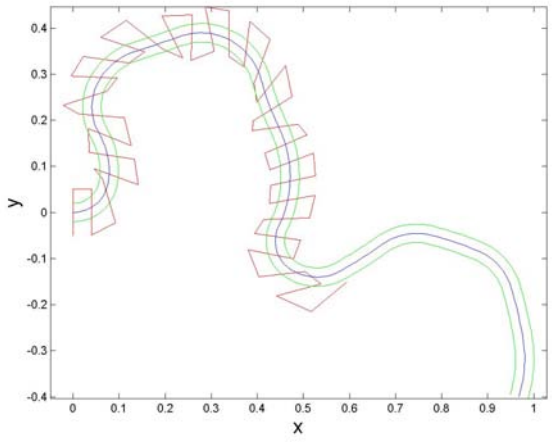

Fig. 4. Effect of step size

IV. Simulations and Experiments

A. Simulation

To initially verify the algorithm we performed a simulation experiment utilizing data from the DNA shown in Figure 2. We note that a plane-fit was performed on the data to remove the offsets in the height measurement which vary across different scan lines. It was assumed that the measurement was corrupted with zero mean Gaussian noise. To estimate the edges of the DNA strand from the height data a maximum likelihood (ML) [14] estimator was used to determine whether a measurement was on the string or off the string. Under the assumption that the string had a rectangular cross section, the ML estimator was a simple threshold test. Because the threshold was set based on the scan line data, it was not sensitive to variations in the height of the sample from scan line to scan line. To prevent chattering due to the fact that the string was not rectangular, a majority rule was used over a small window of measurements around the sample point. Once the edges of the strand were detected, the center was found by taking the midpoint.

In Figure 5 we show the results of the tracking algorithm with the trajectory of the tip shown superimposed on the AFM image. (Superfluous data containing information only about the substrate have been deleted for clarity.) In Figure 6 we show the (simulated) height data acquired by the algorithm. The algorithm tracks the DNA strand fairly well so long as the change in curvature from step to step remains relatively small. The performance of the algorithm in this example appears to be limited primarily by the granularity of the original sampling. So long as the curvature remains fairly small the algorithm is still able to track quite well.

However when the strand has a rapid turn, as on the upper left edge of the strand in Figure 5, the algorithm loses the string. While in practice a large magnitude curvature can be accommodated with smaller steps along the string, in this data set the sampling size is fixed and reducing the step size in the simulation beyond the sampling size does not produce better results.

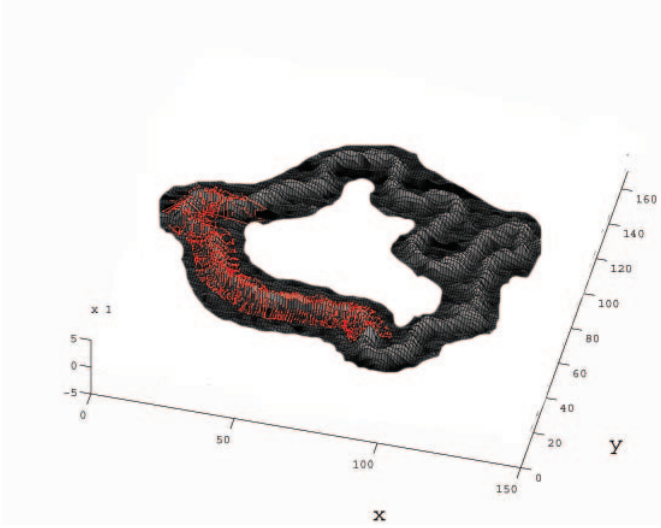

Fig. 5. AFM data and tracking trajectory. Background data was digitally removed to enhance the image contrast.

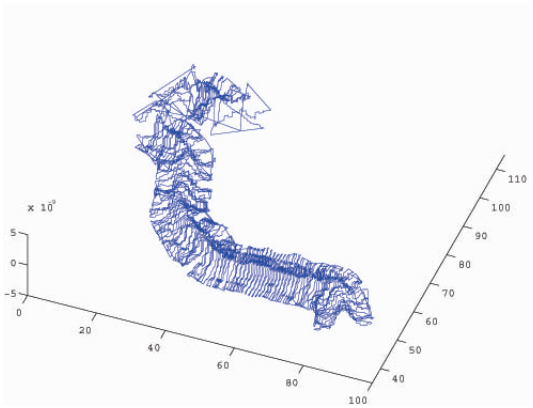

Fig. 6. Data from tracking algorithm alone

B. Experiments

Physical experiments were also performed using a MFP-3D AFM system from Asylum Research. The algorithm was implemented in WaveMetrics' Igor Pro environment and interfaced to the high-level control software of the microscope. While this allowed the algorithm to be implemented quickly, it introduced lengthy communication delays (on the order of 0.5-1 second) between each line scan. As a result the experiments achieved only modest reductions in scan times. However they do serve to illustrate the effectiveness of the technique. The microscope was operated in tapping-mode in air in all experiments.

In Figure 7a we show an image of a carbon nanotube obtained using the traditional raster-scan pattern. The image is 4 μm square with 200 scan lines and 512 points along each line. The image resolution along the nanotube is therefore 20 nm. The tip velocity during the scan was 5 μm/s and the image took 401 seconds to acquire. The same portion of the nanotube was imaged using the local raster-scan algorithm. The algorithm was initialized near the lower end of the nanotube. The scan line length was set to 300 nm with a scan speed of 5 μm/s, as in the traditional raster-scan image. The average step size was 27.3 nm. The resulting image, shown in Figure 7b, was acquired in 197 seconds. The different offsets in the $x - y$ position values was due to the way in which the software stores the positions. The edges of the nanotube were determined using the amplitude signal from the microscope. As the tip encountered the nanotube, the oscillation amplitude decreased until the controller reacted to the change. Similarly, as the tip moved off the tube the oscillation amplitude increased. The edges of the tube were determined by searching the line scan for these peaks. We note that while this approach works well for fairly tall and rigid structures, a more robust detection scheme will likely be required when imaging softer samples. The actual step sizes achieved during the local raster-scan imaging of the nanotube are shown in Figure 7c. Because the low-level controller was designed for the usual raster-scan pattern, it has difficulties when scanning short, arbitrarily oriented lines. This difficulty resulted in uneven step sizes and limits the minimum step size which can be achieved to approximately 10 nm. However, this difficulty is not innate to the actuators and can be overcome through proper controller design.

In this example, the local raster-scan approach approximately halved the imaging time, despite the presence of long communication delays. With a tip speed of 5 μm/s, a scan line of 300 nm would take 60 ms to complete. The local raster-scan algorithm would need to take 200 steps along the 4 μm length of the nanotube in order to match the 20 nm resolution of the image acquired using the standard raster-scan pattern. Neglecting any communication delays, the image would take 12 seconds to complete.

V. Conclusions

For samples which are string-like in nature, the standard raster-scan approach wastes a large amount of time imaging the substrate rather than the sample. In this paper we have presented a high-level algorithm to steer the tip along the sample, thereby imaging only those areas of interest. Modeling the sample as a planar curve whose evolution is given by the planar Frenet-Serret equations, feedback control is used to track the curve. By focusing the resolution of the microscope directly on those areas where it is needed, the time to gather an image is greatly reduced simply by reducing the area that needs to be scanned. In addition, the

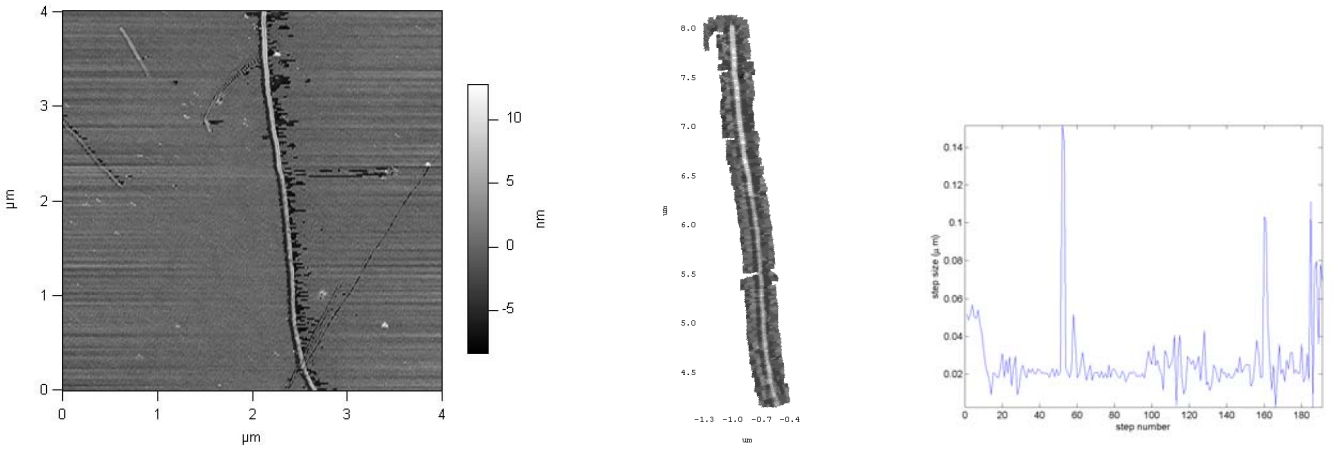

a. Raster-scan image b. Local raster-scan image c. Step sizes

Fig. 7. Carbon nanotube imaged in tapping mode. a. Image acquired using traditional raster-scan pattern. Notice that most of the image is of the substrate. b. Image acquired using local raster-scan. The image contains only data local to the nanotube. c. Step sizes during the local raster-scan.

tip is protected from damage due to debris such as dust particles on the substrate.

We have presented both simulation results and a simple experiment with an atomic force microscope to illustrate the algorithm. Ongoing work is focused on implementing the algorithm on the low-level controller to realize the theoretical reductions in imaging time. Finally, we note that while we have utilized on AFM as the target application in this paper, the method is generally applicable to all scanning probe microscopy technologies.

VI. Acknowledgements

This work was supported in part by the Rowland Institute and by ARO ODDR&E MURI01 Grant No. DAAD19-01-1-0465, (Center for Communicating Networked Control Systems, through Boston University). The authors gratefully acknowledge many fruitful discussions with Roger Brockett concerning this work as well as the technical staff at Asylum Research for their support in developing the software.

References

[1] M. Antognozzi, M.D. Szczelkun, A.D.L. Humphris, and M.J. Miles. Increasing shear force microscopy scanning rate using active quality-factor control. *Applied Physics Letters*, 82(17):2761–2763, 2003.

[2] D. Baselt. Atomic force microscopy. http://stm2.nrl.nvy.mil/how-afm/how-afm.html.

[3] G. Binnig, C.F. Quate, and Ch. Gerber. Atomic force microscope. *Physical Review Letters*, 56(9):930–933, 1986.

[4] G. Binnig, H. Rohrer, Ch. Gerber, and E. Weibel. Tunneling through a controllable vacuum gap. *Applied Physics Letters*, 40(2):178–180, 1982.

[5] E. Calabi, P.J. Olver, C. Shakiban, A. Tannenbaum, and S. Haker. Differential and numerically invariant signature curves applied to object recogonition. *International Journal of Computer Vision*, 26(2):107–135, 1998.

[6] H.C. Crenshaw, C.N. Ciampaglio, and M. McHenry. Analysis of the three-dimensional trajectories of organisms: Estimates of velocity, curvature, and torsion from positional information. *The Journal of Experimental Biology*, 203:961–982, 2000.

[7] A. Daniele, S. Salapake, M.V. Salapaka, and M. Dahleh. Piezoelectric scanners for atomic force microscopes: Design of lateral sensors, identification and control. In *Proceedings of the Americal Control Conference*, pages 253–257, 1999.

[8] U. Durig, D.W. Pohl, and F. Rohner. Near field optical scanning microscopy. *Journal of Applied Physics*, 59(10):3318–3327, 1986.

[9] M. Guthold, M. Bezanilla, D.A. Erie, B. Jenkins, H.G. Hansma, and C. Bustamante. Following the assembly of RNA polymerase-DNA complexes in aqueous solutions with the scanning force microscope. *Proceedings of the National Academy of Sciences*, 91:12927–12931, 1994.

[10] E. Justh and P.S. Krishnaprasad. Equilibria and steering laws for planar formations. *Systems and Control Letters*, 52:25–38, 2004.

[11] S. Kasas, N.H. Thomson, B.L. Smith, H.G. Hansma, X. Zhu, M. Guthold, C. Bustamante, E.T. Kool, M. Kashlev, and P.K. Hansma. *Escherichia coli* RNA polymerase activity observed using atomic force microscopy. *Biochemistry*, 36(3):461–468, 1997.

[12] A. Kornberg and T.A. Baker. *DNA Replication*. W.H. Freeman and Company, 1991.

[13] M. Mertz, O. Marti, and j. Mlynek. Regulation of a microcantilever response by force feedback. *Applied Physics Letters*, 62(19):2344–2346, 1993.

[14] H. Vincent Poor. *An Introduction to Signal Detection and Estimation, Second Edition*. Springer, New York, 1994.

[15] D. R. Sahoo, A. Sebastian, and M. V. Salapaka. Transient-signal-based sample-detection in atomic force microscopy. *Applied Physics Letters*, 83(26):5521–5523, 2003.

[16] G. Schitter, P. Menold, H.F. Knapp, F. Allgöwer, and A. Stemmer. High performance feedback for fast scanning atomic force microscopes. *Review of Scientific Instruments*, 72(8):3320–3327, 2001.

[17] G. Schitter, R.W. Stark, and A. Stemmer. Fast contact-mode atomic force microscopy on biological specimen by model-based control. *Ultramicroscopy*, 100:253–257, 2004.

[18] Z. Shao, J. Mou, D.M. Czajkowsky, J. Yang, and J.Y. Yuan. Biological atomic force microscopy: What is achieved and what is needed. *Advances in Physics*, 45(1):1–86, 1996.

[19] M.B. Viani, T.E Schaeffer, G.T. Paloczi an L.I. Pietrasanta, B.L. Smith, J.B. Thompson, M. Richter, M. Rief, H.E. Gaub, K.W. Plaxco, A.N. Cleland, H.G. Hansma, and P.K. Hansma. Fast imaging and fast force spectroscopy of single biopolymers with a new atomic force microscope designed for small cantilevers. *Review of Scientific Instruments*, 70(11):4300–4303, 1999.

[20] F. Zhang, E. Justh, and P.S. Krishnaprasad. Boundary following using gyroscopic control. In *Proc. of the 43 rd IEEE Conference on Decision and Control, to appear*, 2004.

[21] F. Zhang, A. O'Connor, D. Luebke, and P.S. Krishnaprasad. Experimental study of curvature-based control laws for obstacle avoidance. In *IEEE International Conference on Robotics and Automation*, pages 3849–3954, 2004.

[22] Z. Zhang, P.C. Hammel, and G.J. Moore. Application of a novel rf coil design to the magentic resonance force microscopy. *Review of Scientific Instruments*, 67(9):3307–3309, 1996.